energies

Article

Influence of Different Ambient Temperatures on the Discharge Performance of Square Ternary Lithium-Ion Batteries

Xingxing Wang [1,2], Yujie Zhang [1], Hongjun Ni [1,*], Shuaishuai Lv [1], Fubao Zhang [1], Yu Zhu [1,*], Yinnan Yuan [2] and Yelin Deng [2,*]

[1] School of Mechanical Engineering, Nantong University, Nantong 226019, China; wangxx@ntu.edu.cn (X.W.); 2009310020@stmail.ntu.edu.cn (Y.Z.); lvshuaishuai@ntu.edu.cn (S.L.); zhang.fb@ntu.edu.cn (F.Z.)
[2] School of Rail Transportation, Soochow University, Suzhou 215131, China; yuanyn@suda.edu.cn
* Correspondence: ni.hj@ntu.edu.cn (H.N.); zhu.y@ntu.edu.cn (Y.Z.); yelin.deng@suda.edu.cn (Y.D.)

Abstract: Electric vehicles have a promising development prospect. As its core component, lithium-ion power battery plays a crucial role in different application scenarios. Aiming at the availability and safety of square ternary lithium batteries at different ambient temperatures and different current rates, charge-discharge cycle experiments are carried out to study the voltage, temperature and capacity changes of lithium batteries. The voltage plateau characteristics of lithium batteries under different working conditions are explored. The results show that when discharging at current rates of 0.1C, 0.25C, 0.5C, 0.75C, and 1C under the ambient temperature of −5 °C, 10 °C, 25 °C, and 40 °C, the terminal voltage of the battery changes smoothly during the voltage plateau period, the rise of the surface temperature has not reached the peak value, and the discharge capacity accounts for about 50%. The battery has better working performance. While at the ambient temperature of −20 °C, the discharge capacity accounts for the highest proportion in the stage from the open-circuit voltage to the initial voltage of the plateau period. The research results can provide a reference for the modeling and control strategy design of lithium-ion power batteries in the energy storage system of electric vehicles.

Keywords: electric vehicle; ternary lithium battery; discharge characteristic; piecewise fit; voltage plateau period

check for updates

Citation: Wang, X.; Zhang, Y.; Ni, H.; Lv, S.; Zhang, F.; Zhu, Y.; Yuan, Y.; Deng, Y. Influence of Different Ambient Temperatures on the Discharge Performance of Square Ternary Lithium-Ion Batteries. *Energies* **2022**, *15*, 5348. https://doi.org/10.3390/en15155348

Academic Editors: Saeed Mian Qaisar and Moez Krichen

Received: 28 June 2022
Accepted: 21 July 2022
Published: 23 July 2022

1. Introduction

Electric vehicles have become one of the main means of transportation for building a low-carbon social smart city because of their energy-saving, high-efficiency, and safety features [1–4]. For automotive energy storage systems, the rate of energy storage and long service life (number of cycles), as well as the relatively low cost, are extremely important. There is an opinion [5], that in order to be competitive, the capital cost of energy application storage technology must be equal to or less than $250/kWh on the premise that the life cycle is 15 years or 3900 cycles. Capital cost of $1250/kW or less is desirable. Compared with lead-acid batteries, nickel-metal hydride batteries and other batteries, lithium batteries have the advantages of high voltage platform, small size, light weight, non-polluting, recyclable, high and low temperature adaptability, and long life [6]. Currently, lithium-ion batteries are beginning to dominate in the field of relatively short-term energy storage.

There are two most widely used lithium batteries for electric vehicles, namely lithium iron phosphate batteries and ternary lithium batteries. Table 1 shows the performance comparison between ternary lithium battery and lithium iron phosphate battery [7]. Compared with lithium iron phosphate batteries, ternary lithium batteries have higher energy density and better low-temperature performance, and are more suitable for cold areas [8,9]. The ternary lithium battery refers to the lithium battery whose cathode material is $LiNi_xCo_yMn_{1-x-y}O_2$. Its energy mainly comes from the redox of nickel material, so the higher the nickel content, the higher the energy density of the lithium battery [10–12]. However, the high-nickel ternary lithium battery is unstable at high temperature, and it is easy to generate a cubic rock salt phase that has no lithium-ion deintercalation activity after repeated cycles [13]. This will lead to thinking about the environmental reliability of lithium batteries. Iqbal et al. [14] investigated the stress development under anisotropic lithium flux in graphite particles partially attached to an ionically nonconducting polyvinylidene fluoride (PVDF) binder. It has been shown that due to anisotropic lithium intercalation, the location of maximum stress depends on the particle size and C rate, and mechanical failure can be induced at particle centers or adhesive interfaces according to the size and C rate. Yu et al. [15] study the electrical parameter drift of lithium-ion batteries under high shock and establish a mechanical impact dynamics (MID) model of lithium-ion batteries at high shock times. The effects of parameters such as separator thickness and elastic modulus on the impact resistance of lithium-ion batteries are revealed. Fleischhammer [16] believes that although battery aging does not affect the safety under high-rate discharge, in a high-temperature environment, the aging-induced lithium plating will lead to accelerated heat accumulation, resulting in higher failure risks. However, the country and the market have high demand for high energy density, so high-nickel ternary lithium batteries are still the future development trend.

Table 1. Comparison of parameters between ternary lithium battery and lithium iron phosphate battery.

Type	Specific Energy	Platform Voltage	Advantage	Shortcoming
Lithium iron phosphate battery	140 Wh/kg	3.2 V	High temperature resistance, low cost, impact resistance	Poor consistency, poor low temperature performance
Ternary lithium battery	220 Wh/kg	3.7 V	High specific energy, low temperature resistance, good discharge linearity	Poor thermal stability

At this stage, a large number of experimental schemes using lithium iron phosphate batteries as the research object have basically matured, providing a certain reference for the experiments of ternary lithium batteries with wide temperature range and multiple current rates. Panchal et al. [17] take the aluminum laminated prismatic battery composed of 20 Ah lithium iron phosphate cathode material as the research object. The changes in battery heat generation rate and discharge capacity are studied through the discharge rates of 1C, 2C, 3C, and 4C and the boundary conditions of 5 °C, 15 °C, 25 °C, and 35 °C. The results show that the maximum heat generation at 4C discharge rate and 5 °C boundary condition is 7 times the minimum heat generation at 1C discharge rate and 35 °C boundary condition. At the same time, it is found that the increase of the heating rate and the decrease of the discharge capacity are consistent with the increase of the discharge rate. Chen et al. [18] study the effect of temperature on the median discharge voltage of lithium iron phosphate power batteries, and study the effects of high temperature and low temperature on the performance of lithium iron phosphate power batteries in terms of the median voltage of battery discharge. The low temperature has a great influence on the battery performance, and the battery performance does not change significantly at high temperature. The battery performance begins to decline when the temperature is above 50 °C. The most ideal working temperature is between 20 and 50 °C. Wang [19] conducts high-rate (1C, 2C, 3C) charge-discharge experiments at 25 °C, 10 °C, 0 °C, −10 °C, and −20 °C, respectively. Experiments show that the charge-discharge time and capacity of lithium iron phosphate batteries decrease with the decrease of ambient temperature, and the internal temperature and internal strain increase with the decrease of ambient temperature. When the ambient temperature drops by about 10 °C, the charge-discharge time is correspondingly reduced by about 10%. At 25 °C, 10 °C, and 0 °C, the battery exhibits a flat and long voltage plateau, but when the temperature is −10 °C and −20 °C, the voltage rebounds at the initial stage of charge and discharge. It can be found that the piecewise performance of lithium iron phosphate batteries has made some progress. An et al. [20] study the effect of temperature on the capacity decay and battery aging of ternary lithium batteries, and find that structures such as electrode thickness and porosity have a significant impact on battery heat generation and capacity changes. Gu et al. [21] study the charge-discharge behavior of ternary lithium batteries in a low temperature environment and find that when the ambient temperature drops from 55 °C to 0 °C and −20 °C, respectively, the coulombic efficiency of lithium batteries drops from 100% to 96% and 64%. The discharge voltage decreases from 3.11 V at 55 °C to 2.62 V at −20 °C. It shows that low temperature environment has a significant impact on the energy storage efficiency of lithium batteries. Compared with lithium iron phosphate batteries, there are fewer systematic experiments on the subsection research on the discharge characteristics of ternary lithium batteries, and it is difficult to meet the needs of electric vehicles to seek the optimal working stage of lithium batteries under different working conditions [22–24].

For lithium-ion batteries with the same cathode material, due to various factors such as different reaction potentials of each element, different element concentration ratios in the battery reaction, and differences in processing techniques, the plateau characteristics of different batteries will also be different. Bloom et al. [25] use the differential voltage method to compare and analyze the charge-discharge process and capacity decay process of lithium-ion batteries. The peak values of the dQ/dV curve reflect the negative electrode lithium intercalation platform of batteries with different electrolyte ratios. Jia [26] studies the change rule of the inflection point between each reaction stage of lithium-ion battery, and finds that the inflection point position of the constant current charging curve of the same environment and the same rate is almost the same, and proposes a battery capacity estimation scheme based on the constant current charging curve platform of lithium battery. Zhang et al. [27] prepare $LiFePO_4/C$ cathode materials by different methods, and find that due to the difference in the fabrication process of batteries of the same specification, the plateau voltage difference of different samples reaches 70 mV when charging and discharging at 0.1C rate, and the voltage plateau time is also different.

Lithium battery is a complex nonlinear dynamic system. Its regular characteristics should be summed up through multi-angle test experiments, and then its general physical model can be established by parameter identification [28–30]. The research object of this paper is the square high-nickel ternary power lithium battery. Aiming at its usability and safety under different ambient temperatures during cascade utilization, charge-discharge cycle experiments at different current rates are carried out to observe the voltage, temperature and capacity changes of the lithium battery. The voltage plateau characteristics of ternary lithium batteries in different working states are explored, which lays a foundation for the modeling and control strategy design of lithium-ion power batteries in electric vehicle energy storage systems.

The rest of the paper is organized as follows. After a general introduction, the object, method and equipment of the experiment are presented in Section 2. Then, Section 3 describes the changing trend of voltage, temperature, and capacity of lithium battery during the discharge process. In Section 4, segmental fitting is carried out for the voltage plateau period, and the voltage, temperature, capacity, and energy of this stage are analyzed and compared. The Section 5 is made for resuming this work and for presenting future endeavors.

2. Materials and Methods

2.1. Object

A common lithium-ion battery consists of a lithium compound-based cathode, a carbon-based anode, an electrolyte, and a separator. Typically, cathode material and anode material are coated on aluminum and copper foils, respectively. A porous polymer separator immersed in the electrolyte and sandwiched between the anode and cathode prevents the two electrodes from short-circuiting (Figure 1a). As shown in Figure 1b, Li ions undergo cycles of intercalation and deintercalation, and shuttle in the electrolyte as charge carriers in the internal circuit. With the intercalation and deintercalation of lithium-ions, a redox reaction occurs on the electrode, and the generated electrons move directionally through the external circuit to form a current. The research object selected in this paper is the square ternary lithium battery (produced by Contemporary Amperex Technology Co., Ltd., Ningde, China) with a rated voltage of 3.65 V and a rated capacity of 40 Ah. The relevant technical parameters are shown in Table 2.

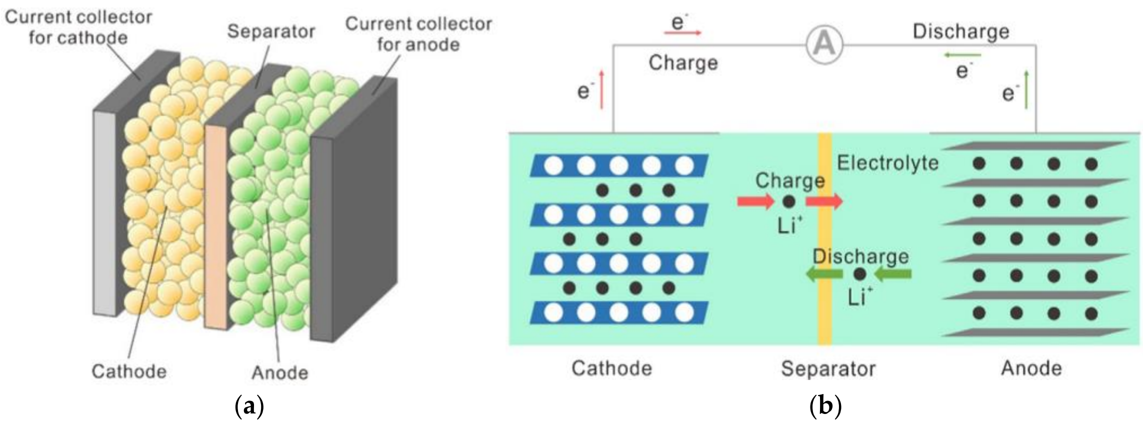

Figure 1. (**a**) Schematic diagram of lithium battery structure. Reprinted with authorization of [31]. Copyright: 2017, Elsevier; (**b**) Working principle diagram of lithium battery. Reprinted with authorization of [32]. Copyright: 2018, Elsevier.

Table 2. Lithium battery technical parameters.

Performance	Parameter
Rated voltage (V)	3.65
Operating voltage (V)	2.75–4.2
Rated capacity (Ah)	40
Standard internal resistance (mΩ)	0.7
Specific energy (Wh/kg)	206
Size (mm)	148 × 91 × 27
Weight (kg)	0.7

2.2. Method

During the experiment, it is necessary to carry out experimental tests on lithium-ion batteries under the conditions of low power output and large power output, and obtain the battery output characteristics under different conditions to provide an experimental basis for formulating battery energy supply strategies [33,34].

The specific experimental process is shown in Figure 2. First, put the lithium battery at −20 °C, −5 °C, 10 °C, 25 °C, and 40 °C ambient temperature for 10 h, and then charge it with a constant current of 1C to the end-of-charge voltage (4.2 V), and then switch to constant-voltage charging. Stop charging when the charging current drops to 0.05C. After standing, discharge with different currents of 0.1C, 0.25C, 0.5C, 0.75C, and 1C to the end-of-discharge voltage (2.75 V), and then charge to the end-of-charge voltage for charge-discharge experiments [35].

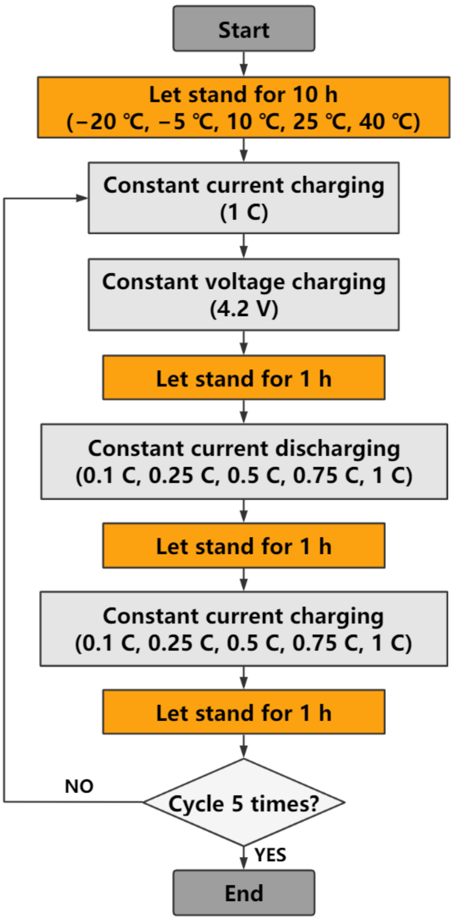

Figure 2. Experimental flow chart.

2.3. Platform

The experimental platform consists of a programmable constant temperature and humidity chamber (Sanwood, Dongguan, China), CT5002A battery test system (LANHE, Wuhan, China), corresponding detection unit, host computer, and monitoring software. The constant temperature and humidity chamber and battery test system are shown in Figure 3.

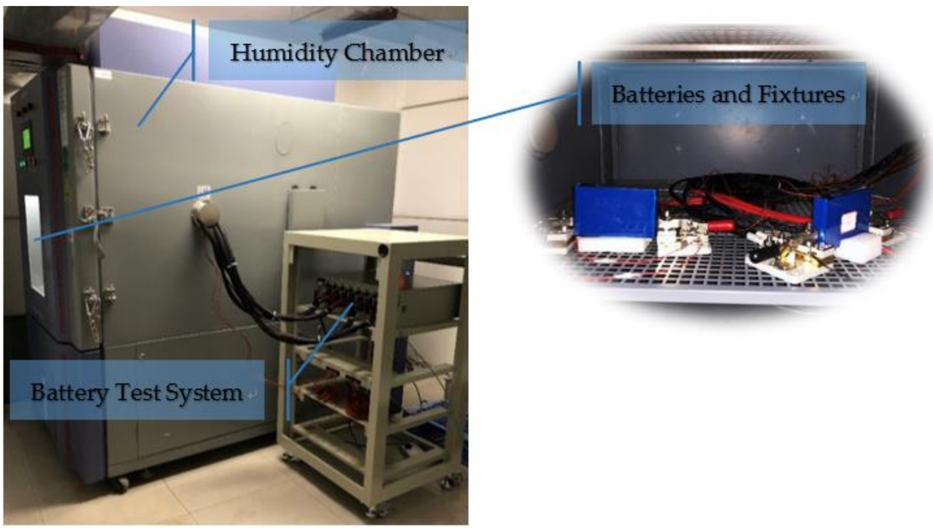

Figure 3. Experiment platform.

3. Results

Since the charging and discharging process and its balance of lithium batteries are managed by the battery management system in the actual use process, it is assumed that there is no difference between each lithium battery in this experiment, and the balance in the charging and discharging process is ignored [36].

3.1. Influence of Different Ambient Temperatures on Battery Discharge Voltage

As shown in Figure 4, the battery voltage changes with time during discharge at different ambient temperatures of −20 °C, −5 °C, 10 °C, 25 °C, and 40 °C at the same current rate. It can be seen that the change rule of the battery voltage at any rate is that the voltage drops rapidly in the period before the battery starts to discharge. As the discharge time goes on, the battery voltage has a relatively gentle change process. At the end of the discharge, the terminal voltage drops significantly again.

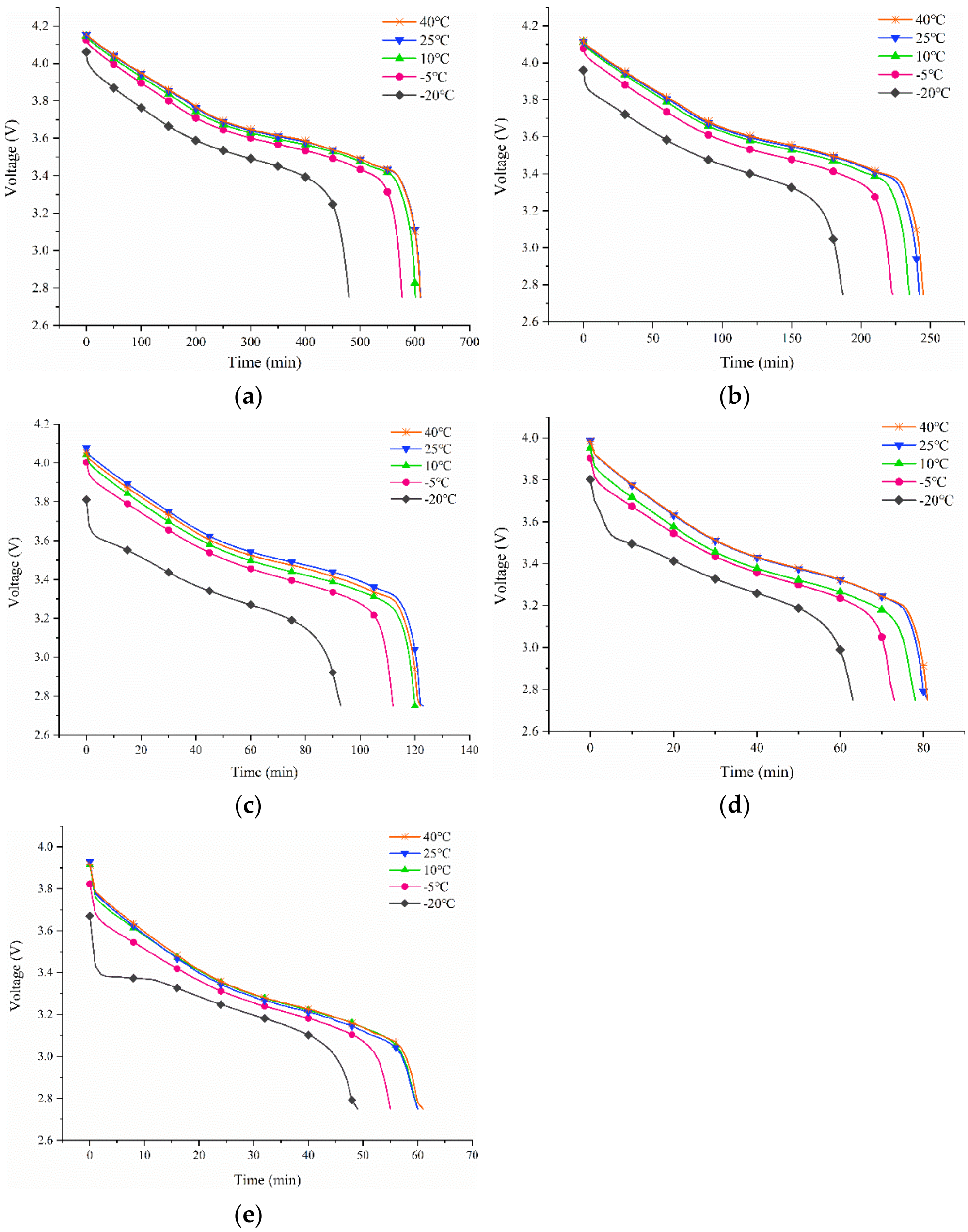

Figure 4. Discharge voltage change curve: (**a**) 0.1C discharge rate; (**b**) 0.25C discharge rate; (**c**) 0.5C discharge rate; (**d**) 0.75C discharge rate; (**e**) 1C discharge rate.

At the same time, due to the existence of ohmic voltage drop and activation polarization, the terminal voltage at the initial stage of discharge will have a transition-like sudden drop at the 4.2 V platform. As the ambient temperature is higher and the discharge rate is smaller, the initial terminal voltage is also higher. When the ambient temperature is 40 °C and the discharge rate is 0.1C, the initial terminal voltage reaches the maximum value of 4.1560 V, with a decrease of 1.05%. At the ambient temperature of −20 °C and the discharge rate of 1C, the initial terminal voltage reaches the minimum value of 3.6703 V, which is nearly 0.5 V away from the maximum value, with a decrease of 12.61%.

In addition, as the ambient temperature decreases and the discharge rate increases, the discharge speed of the battery is accelerated, and the discharge time is shorter. At the same current rate, when the ambient temperature is 10 °C and above, the voltage trend is roughly the same, and the voltage curves at 25 °C and 40 °C basically overlap. When the ambient temperature reaches −5 °C, the curve shifts significantly, and when the ambient temperature is −20 °C, the curve changes greatly. When the ambient temperature is 10 °C, and above, the discharge time of 0.1C, 0.25C, 0.5C, 0.75C, and 1C is approximately 600 min, 240 min, 120 min, 80 min, and 60 min. While at the ambient temperature of −20 °C, the discharge time is 480 min, 187 min, 93 min, 63 min, and 49 min, respectively.

3.2. Influence of Different Ambient Temperatures on the Temperature Rise during Battery Discharge

Figure 5 shows the trend of the battery surface temperature changing with time during discharge at different ambient temperatures of −20 °C, −5 °C, 10 °C, 25 °C, and 40 °C at the same current rate. It can be observed that the overall temperature change curve of the battery surface shows a trend of first rising, then falling, and then rising. Due to the existence of polarization at the beginning and end of discharge, the surface temperature of lithium batteries rises rapidly. In the voltage plateau period, the reaction is slow, and the temperature drops to a certain extent. When the discharge rate increases to 0.75C and 1C, the plateau period is short, and the battery surface temperature does not drop significantly or shows a slow rise [32].

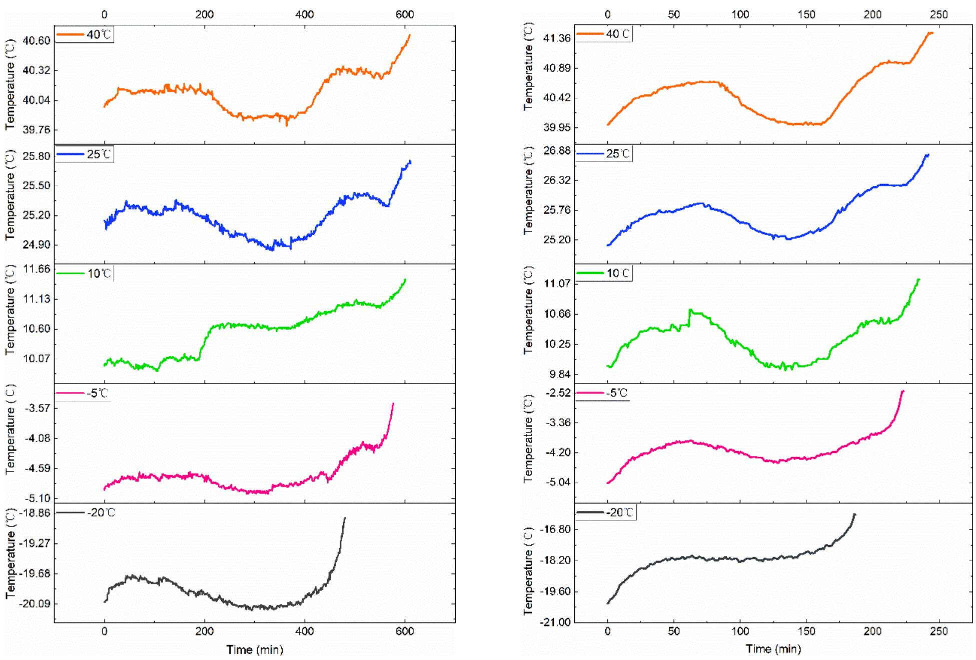

(**a**) (**b**)

Figure 5. *Cont.*

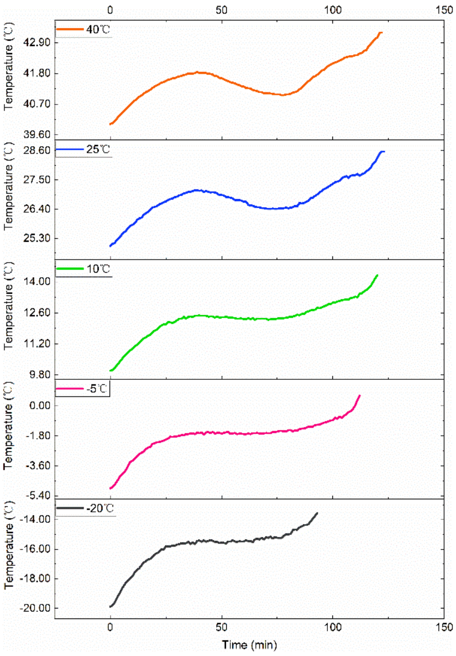

(**c**)

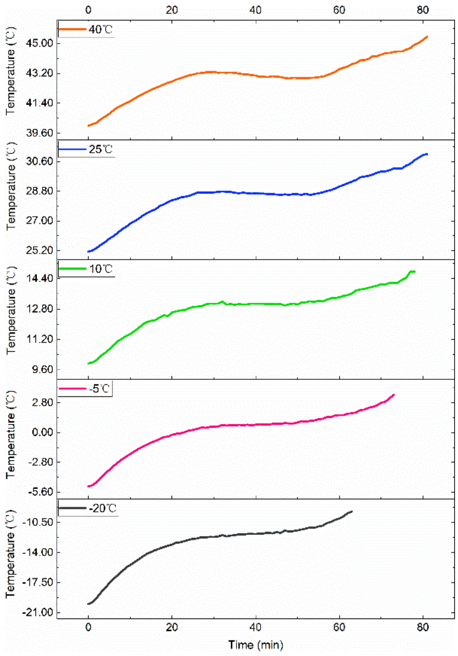

(**d**)

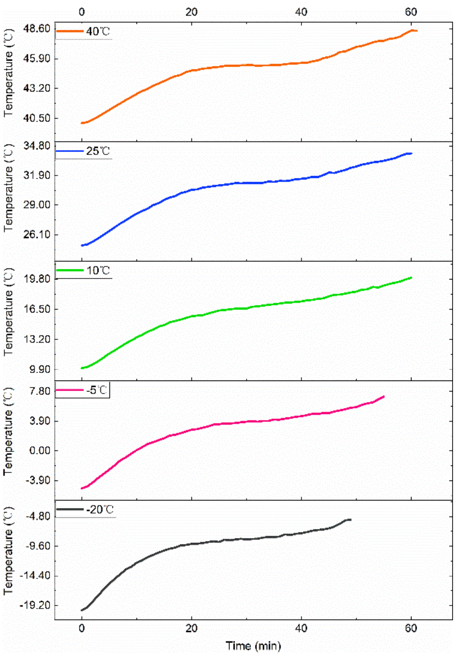

(**e**)

Figure 5. The temperature change curve of the battery surface during discharge: (**a**) 0.1C discharge rate; (**b**) 0.25C discharge rate; (**c**) 0.5C discharge rate; (**d**) 0.75C discharge rate; (**e**) 1C discharge rate.

3.3. Influence of Different Ambient Temperatures and Discharge Rates on Battery Capacity

Figure 6 shows the comparison of discharge capacity under different experimental conditions. It can be seen that the discharge process generally follows the law that the higher the ambient temperature, the greater the discharge capacity. However, the maximum capacity differences between groups at the same ambient temperature and different current are 1.34 Ah, 2.19 Ah, 1.27 Ah, 0.98 Ah, and 0.63 Ah, respectively. Additionally, the maximum difference is about 5% of the nominal capacity, indicating that the impact of small current discharge below 1C rate on the battery capacity change at the same ambient temperature is relatively small, and the impact of a wider discharge rate range still needs further research.

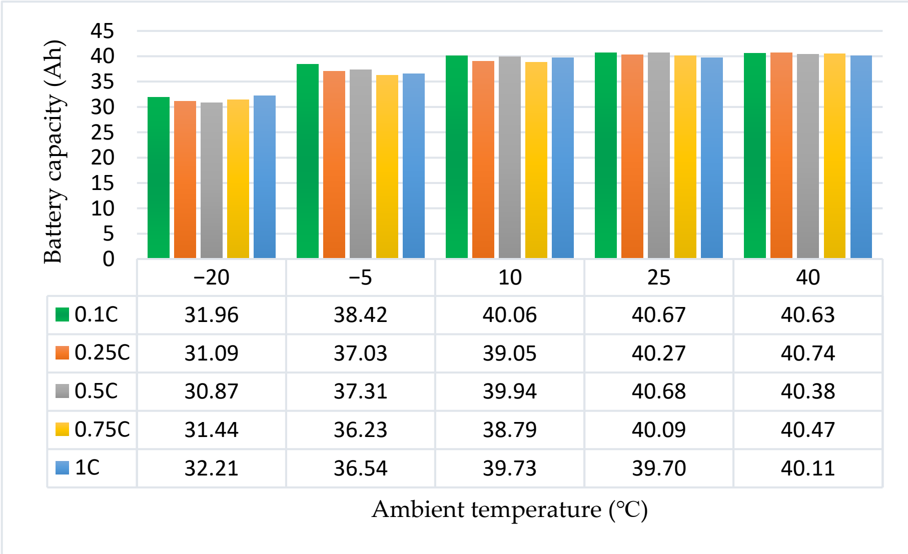

Figure 6. Discharge capacity comparison chart.

At the ambient temperatures of 10 °C, 25 °C, and 40 °C, the discharge capacity can basically reach the nominal capacity of 40 Ah. When the ambient temperature drops to −5 °C, the capacity decreases to a certain extent. It can still reach 38.42 Ah at a low current of 0.1C, while it has dropped to a minimum of 36.23 Ah at 0.75C. When the ambient temperature drops to −20 °C, the capacity drops significantly to about 80% of the nominal capacity. There are many reasons for the significant reduction in the capacity of lithium-ion batteries at low temperatures. The physicochemical function of the electrolyte and the composition of the electrolyte have an important impact on the low-temperature function of the battery. In a lithium-ion battery in a low temperature state, the viscosity of the electrolyte increases, so the ion conduction speed in the electrolyte decreases. This phenomenon causes a mismatch between the external circuit and the internal electron transfer speed, resulting in serious polarization of the battery. On the other hand, the diffusion coefficient of active substances in low temperature environment decreases, the charge transfer resistance increases greatly, and the discharge capacity of the battery decreases greatly [37].

4. Discussion

4.1. Overview and Division Method of Voltage Plateau Period

The change of the voltage platform during the discharge process of the lithium battery is mainly affected by the ohmic resistance and the polarization resistance, and the polarization resistance is caused by the internal polarization phenomenon of the lithium battery. The polarization phenomenon is divided into activation polarization and concentration polarization. In a physical sense, active polarization can be understood as the rate of chemical reaction on the surface of the active electrode particles is slightly slower than the electron migration rate, so the current potential on the surface of the electrode particles is shifted from the equilibrium potential and causes active polarization, which is manifested as a change in the transition of the battery terminal voltage at the initial discharge. The polarization phenomenon is mainly determined by the activation energy of the electrochemical reaction of the electrode. The phenomenon of concentration polarization, as the name suggests, is caused by the concentration difference. During the discharge process of the lithium battery, since the migration rate of Li^+ inside the electrode particle is much smaller than that of the electrolyte, the transfer rate of Li^+ inside the electrode particle is far less than the electrochemical reaction rate occurring on its surface. It causes the phenomenon of concentration polarization and further exacerbates the deviation of the positive and negative electrode potentials from the equilibrium potential, which is manifested as a rapid change in the terminal voltage at the initial period and the end period of the discharge process of the lithium battery.

It can be found from the experimental results that there is a relatively gentle change process between the initial stage and the end stage of the lithium battery voltage curve at any rate. Different from the lithium iron phosphate battery, the reaction platform period of the ternary lithium battery is shorter, and the whole curve is not as flat as the voltage curve of the lithium iron phosphate battery. This is because the lithium intercalation process from $FePO_4$ to $LiFePO_4$ in the lithium iron phosphate battery is long, and the Mn, Ni, and Co elements contained in the ternary lithium battery make it appear in multiple reaction platforms with significantly different potentials. As a result, the voltage plateau reaction trend of ternary lithium battery gradually decreases [38].

The existence of a voltage plateau means that there are turning points of the curve. The entire discharge curve is analyzed through the concavity and convexity of the curve. The inflection point entering the platform reaction stage is a concave curve, that is, the point at which the second derivative is greater than zero and the maximum value of the third derivative corresponds; the inflection point at the end of the platform and entering the next reaction stage is a convex curve, that is, the point at which the second derivative is less than zero and the maximum value of the third derivative corresponds. Based on this, the positions of the inflection points are determined and after some optimization and correction, the discharge curve is divided into three periods: the initial period, the voltage plateau period, and the end period. Segmented fitting is performed for the voltage plateau period to obtain the fitting graph and fitting equation, and to carry out further analysis [39].

4.2. Influence Rule of Different Ambient Temperatures on Voltage Plateau Period

4.2.1. 0.1C Discharge

Figure 7 shows the curve fitting diagram and fitting equation of the battery terminal voltage plateau period at the discharge rate of 0.1C. It can be seen that the voltage plateau period under each temperature environment can be fitted to a linear regression equation, and the coefficient of determination R^2 is greater than 0.98. When the ambient temperature is -5 °C, 10 °C, 25 °C, and 40 °C, the slope of the linear equation is about -8×10^{-4}. Δx increases in turn, and is basically maintained at about 300. When the ambient temperature is -20 °C, the slope of the linear equation is -9.37×10^{-4} and Δx is 164. Consistent with the trend of the overall discharge curve, the voltage plateau period has a larger change range and a shorter time at low temperature.

The voltage variation interval diagram of the voltage plateau period during 0.1C discharge is shown in Figure 8. Based on this, the changes of battery surface temperature and discharge capacity during the period when the voltage is reduced from 3.7 V to 3.4 V at the ambient temperature of -5 °C, 10 °C, 25 °C, and 40 °C are studied. It is found that the temperature change is stable and the peak temperature is avoided. The discharge capacities are 23.27 Ah, 23.93 Ah, 23.39 Ah, and 22.86 Ah, respectively, accounting for 60.57%, 59.74%, 57.51%, and 56.26% of the total discharge capacities, all of which are greater than 55%. It shows that the working performance of the battery during the voltage platform period is excellent, which provides a basis for allocating the best working section of the battery when establishing the physical model and designing the control strategy. At the same time, the discharge capacity during the period when the voltage is reduced from 3.53 V to 3.37 V at the ambient temperature of -20 °C is studied. It is found that the discharge capacity only accounts for 34.21%, which is lower than 52.56% in the initial stage (open-circuit voltage discharge to 3.53 V), indicating that the voltage plateau period is short and the performance is not outstanding at low temperature.

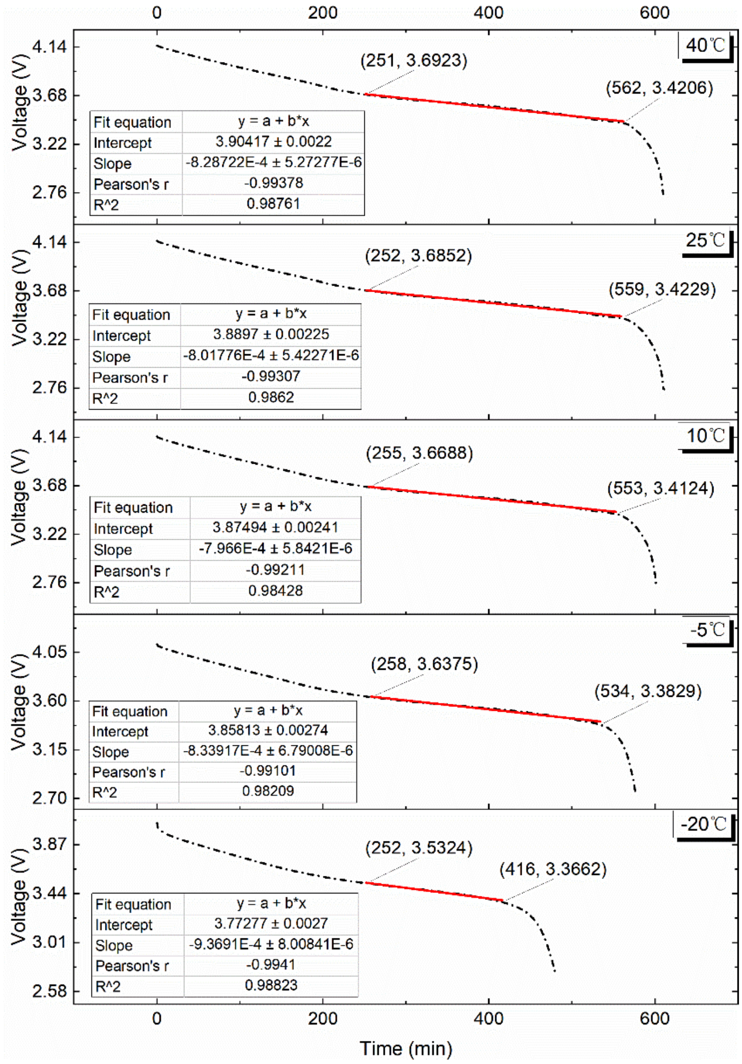

Figure 7. Influence rule of different ambient temperatures on voltage plateau period during 0.1C discharge.

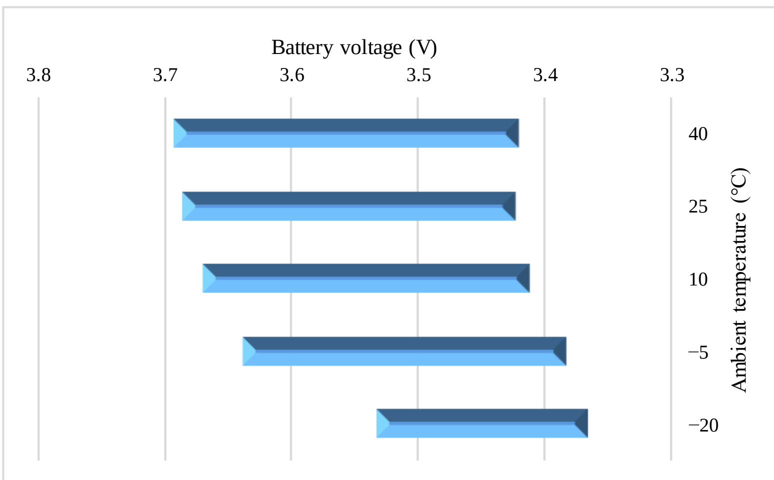

Figure 8. The voltage variation interval diagram of the voltage plateau period during 0.1C discharge.

4.2.2. 0.25C Discharge

Figure 9 shows the curve fitting diagram and fitting equation of the battery terminal voltage plateau period when discharging at a current rate of 0.25C. It can be seen that the voltage plateau period under each temperature environment can be fitted to a linear regression equation, and the coefficient of determination R^2 is greater than 0.98. When the ambient temperature is −5 °C, 10 °C, 25 °C, and 40 °C, the slope of the linear equation is about -2×10^{-3}. Δx increases in turn, and is basically maintained at about 100. When the ambient temperature is −20 °C, the slope of the linear equation is -2.54×10^{-3} and Δx is 58. Consistent with the trend of the overall discharge curve, the voltage plateau period has a larger change range and a shorter time at low temperature.

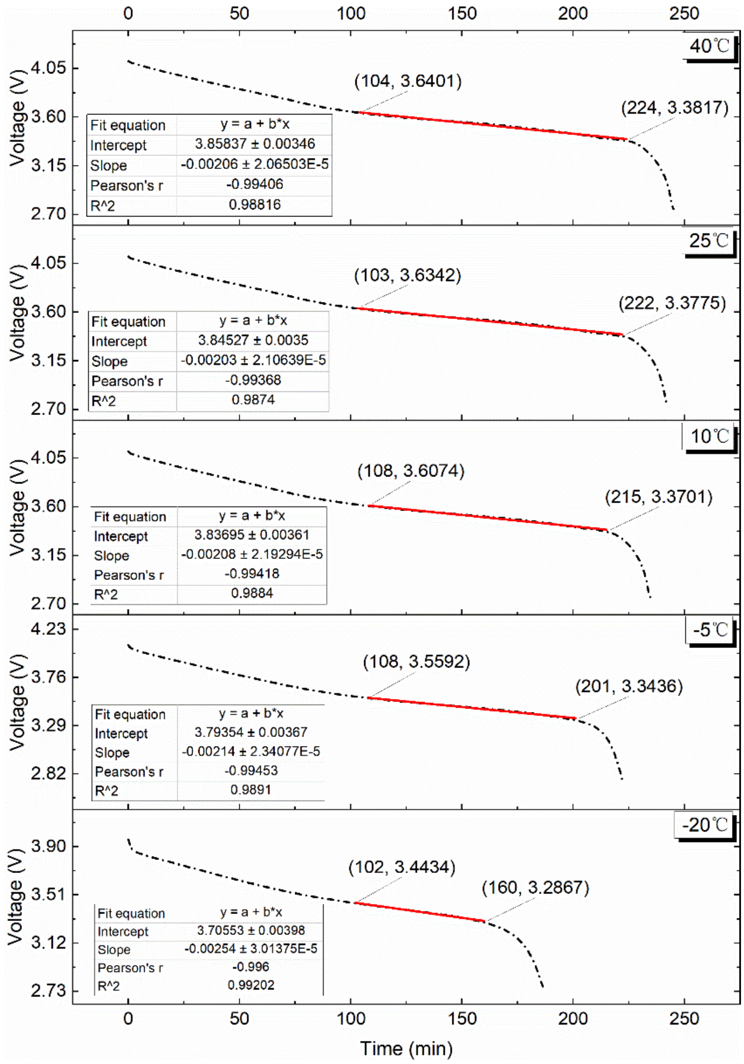

Figure 9. Influence rule of different ambient temperatures on voltage plateau period during 0.25C discharge.

The voltage variation interval diagram of the voltage plateau period during 0.25C discharge is shown in Figure 10. Based on this, the changes of battery surface temperature and discharge capacity during the period when the voltage is reduced from 3.65 V to 3.35 V at the ambient temperature of −5 °C, 10 °C, 25 °C, and 40 °C are studied. It is found that the temperature change is stable and the peak temperature is avoided. The discharge capacities are 20 Ah, 21.33 Ah, 21.84 Ah, and 22 Ah, respectively, accounting for 54.01%, 54.62%, 54.23%, and 54.02% of the total discharge capacities, all of which are greater than 50%. It shows that the working performance of the battery during the voltage platform period is excellent, which provides a basis for allocating the best working section of the battery when establishing the physical model and designing the control strategy. Meanwhile, the discharge capacity during the period when the voltage is reduced from 3.44 V to 3.29 V at the ambient temperature of −20 °C is studied. It is found that the discharge capacity only accounts for 31.09%, which is lower than 54.68% in the initial stage (open-circuit voltage discharge to 3.44 V), indicating that the voltage plateau period is short and the performance is not outstanding at low temperature.

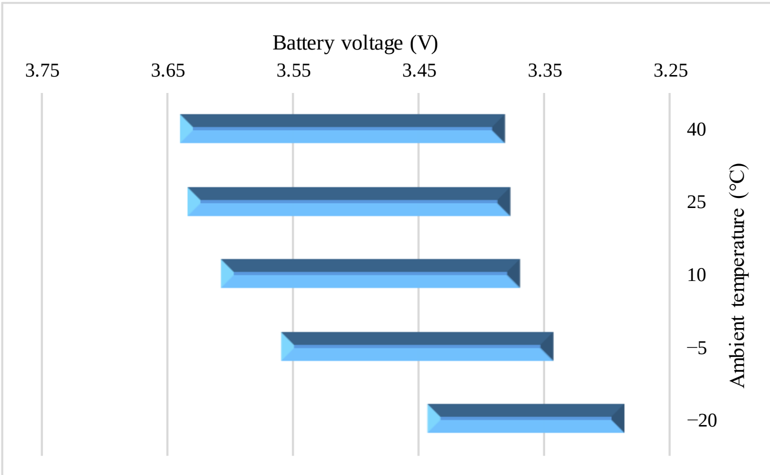

Figure 10. The voltage variation interval diagram of the voltage plateau period during 0.25C discharge.

4.2.3. 0.5C Discharge

Figure 11 shows the curve fitting diagram and fitting equation of the battery terminal voltage plateau period when discharging at a current rate of 0.5C. It can be found that the voltage plateau period under each temperature environment can be fitted to a linear regression equation, and the coefficient of determination R^2 is greater than 0.98. When the ambient temperature is −5 °C, 10 °C, 25 °C, and 40 °C, the slope of the linear equation is about -4×10^{-3}. Δx increases in turn, and is basically maintained at about 50. When the ambient temperature is −20 °C, the slope of the linear equation is -5.3×10^{-3} and Δx is 28. Consistent with the trend of the overall discharge curve, the voltage plateau period has a larger change range and a shorter time at low temperature.

The voltage variation interval diagram of the voltage plateau period during 0.5C discharge is shown in Figure 12. Based on this, the changes of battery surface temperature and discharge capacity during the period when the voltage is reduced from 3.55 V to 3.25 V at the ambient temperature of −5 °C, 10 °C, 25 °C, and 40 °C are studied. It is found that the temperature change is stable and the peak temperature is avoided. The discharge capacities are 20.01 Ah, 21 Ah, 19.67 Ah, and 20.34 Ah, respectively, accounting for 53.63%, 52.58%, 48.35%, and 50.37% of the total discharge capacities, all of which are about 50%. It shows that the working performance of the battery during the voltage platform period is excellent, which provides a basis for allocating the best working section of the battery when establishing the physical model and designing the control strategy. Meanwhile, the discharge capacity during the period when the voltage is reduced from 3.31 V to 3.15 V at the ambient temperature of −20 °C is studied. It is found that the discharge capacity only accounts for 30.24%, which is lower than 56.15% in the initial stage (open-circuit voltage discharge to 3.31 V), indicating that the voltage plateau period is short and the performance is not outstanding at low temperature.

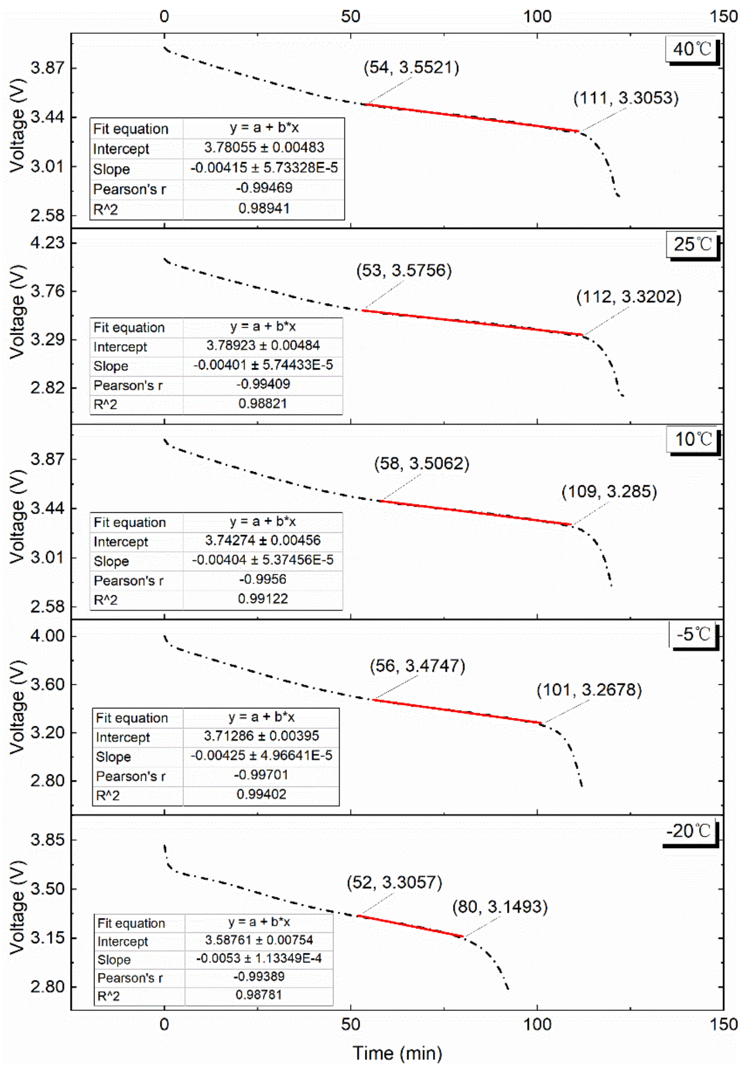

Figure 11. Influence rule of different ambient temperatures on voltage plateau period during 0.5C discharge.

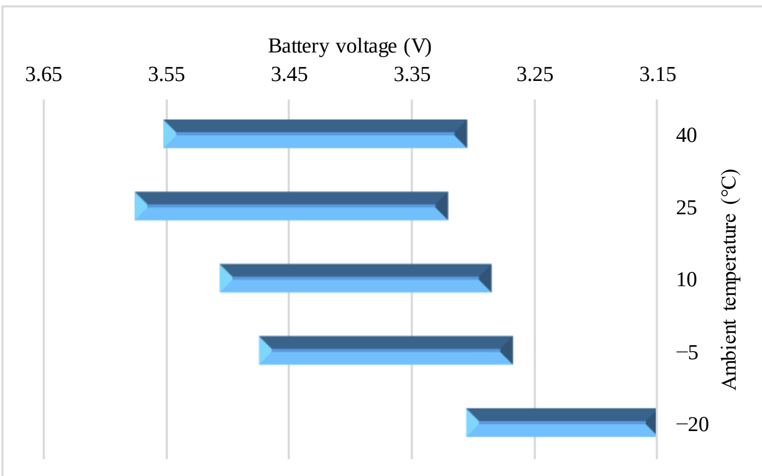

Figure 12. The voltage variation interval diagram of the voltage plateau period during 0.5C discharge.

4.2.4. 0.75C Discharge

Figure 13 shows the curve fitting diagram and fitting equation of the battery terminal voltage plateau period when discharging at a current rate of 0.75C. It can be seen that the voltage plateau period under each temperature environment can be fitted to a linear regression equation, and the coefficient of determination R^2 is greater than 0.98. When the ambient temperature is −5 °C, 10 °C, 25 °C, and 40 °C, the slope of the linear equation is about -6.2×10^{-3}. Δx increases in turn, and is basically maintained at about 35. When the ambient temperature is −20 °C, the slope of the linear equation is -7.3×10^{-3} and Δx is 22. Consistent with the trend of the overall discharge curve, the voltage plateau period has a larger change range and a shorter time at low temperature.

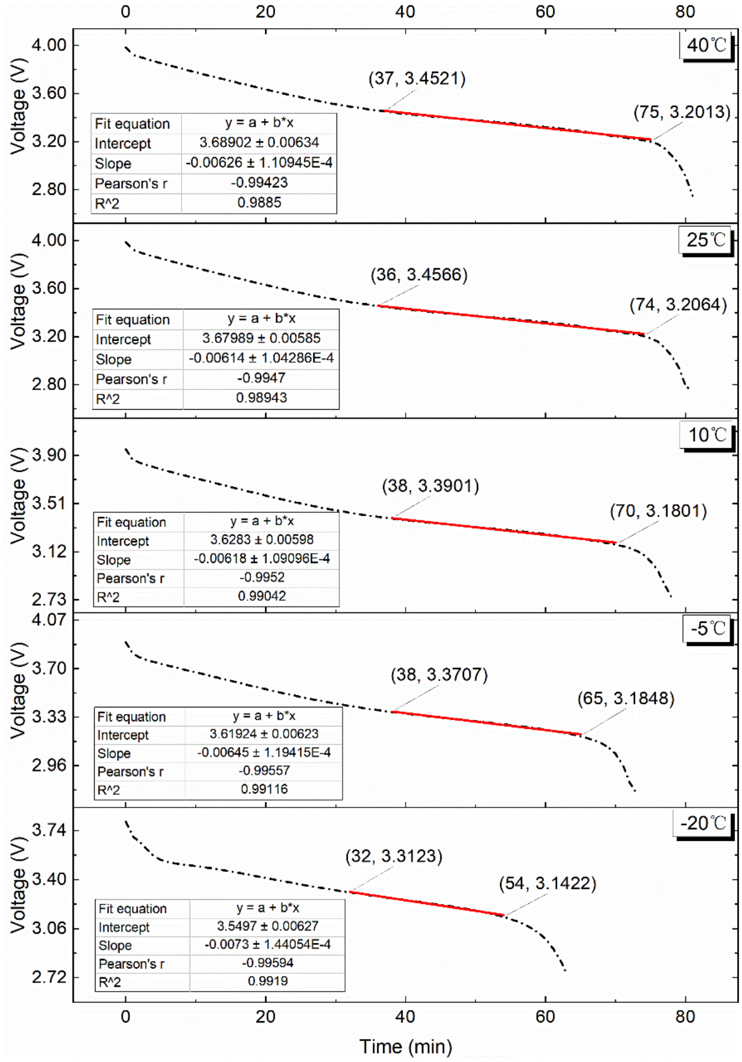

Figure 13. Influence rule of different ambient temperatures on voltage plateau period during 0.75C discharge.

The voltage variation interval diagram of the voltage plateau period during 0.75C discharge is shown in Figure 14. According to this, the changes of battery surface temperature and discharge capacity during the period when the voltage is reduced from 3.45 V to 3.2 V at the ambient temperature of −5 °C, 10 °C, 25 °C, and 40 °C are studied. It is found that the temperature change is stable and the peak temperature is avoided. The discharge capacities are 18 Ah, 19.5 Ah, 19 Ah, and 19 Ah, respectively, accounting for 49.68%, 50.27%, 47.39%, and 46.95% of the total discharge capacities, all of which are about 50%. It shows that the working performance of the battery during the voltage platform period is excellent, which provides a basis for allocating the best working section of the battery when establishing the physical model and designing the control strategy. At the same time, the discharge capacity during the period when the voltage is reduced from 3.31 V to 3.14 V at the ambient temperature of −20 °C is studied. It is found that the discharge capacity only accounts for 34.99%, which is lower than 50.89% in the initial stage (open-circuit voltage discharge to 3.31 V), indicating that the voltage plateau period is short and the performance is not outstanding at low temperature.

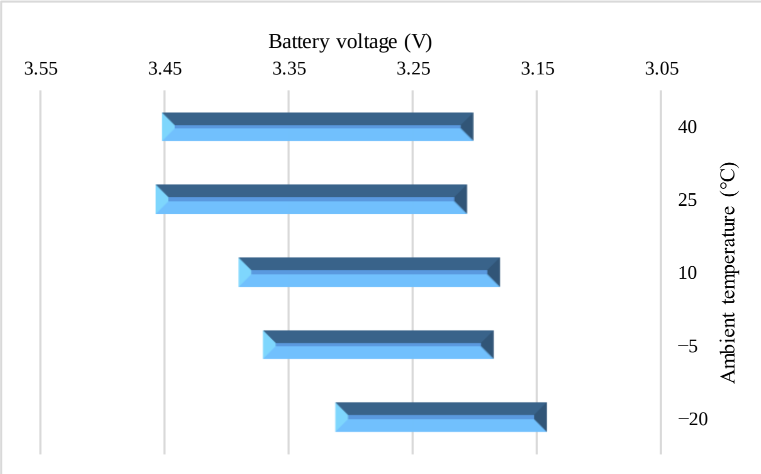

Figure 14. The voltage variation interval diagram of the voltage plateau period during 0.75C discharge.

4.2.5. 1C Discharge

Figure 15 shows the curve fitting diagram and fitting equation of the battery terminal voltage plateau period at the discharge rate of 1C. It can be seen that the voltage plateau period under each temperature environment can be fitted to a linear regression equation, and the coefficient of determination R^2 is greater than 0.98. When the ambient temperature is −5 °C, 10 °C, 25 °C, and 40 °C, the slope of the linear equation is about -8×10^{-3}. Δx increases in turn, and is basically maintained at about 25. When the ambient temperature is −20 °C, since the electrolyte is in a solidified or semi-solidified state at low temperature, the conductivity of the electrolyte decreases, and the voltage plateau drops rapidly at the initial stage of discharge. As the discharge process progresses, according to the experimental results, it is observed that the surface temperature of the battery continues to rise, and the generated heat melts the electrolyte, which increases the conductivity of the electrolyte, reduces the resistance to electron flow, and slows down the rate of change of the discharge platform. After reaching the normal discharge plateau, the discharge curve including the voltage plateau period tends to be consistent, the slope of the linear equation is -9×10^{-3}, and Δx is 28.

The voltage variation interval diagram of the voltage plateau period during 1C discharge is shown in Figure 16. Based on this, the changes of battery surface temperature and discharge capacity during the period when the voltage is reduced from 3.3 V to 3.05 V at the ambient temperature of −5 °C, 10 °C, 25 °C, and 40 °C are studied. It is found that the temperature change is stable and the peak temperature is avoided. The discharge capacities are 19.33 Ah, 20.66 Ah, 20 Ah, and 18.67 Ah, respectively, accounting for 52.90%, 52.00%, 50.38%, and 46.55% of the total discharge capacities, all of which are about 50%. It shows that the working performance of the battery during the voltage platform period is excellent, which provides a basis for allocating the best working section of the battery when establishing the physical model and designing the control strategy. Meanwhile, the discharge capacity during the period when the voltage is reduced from 3.36 V to 3.1 V at the ambient temperature of −20 °C is studied. It is found that the discharge capacity accounts for 57.96% of the stable discharge stage including the voltage plateau period.

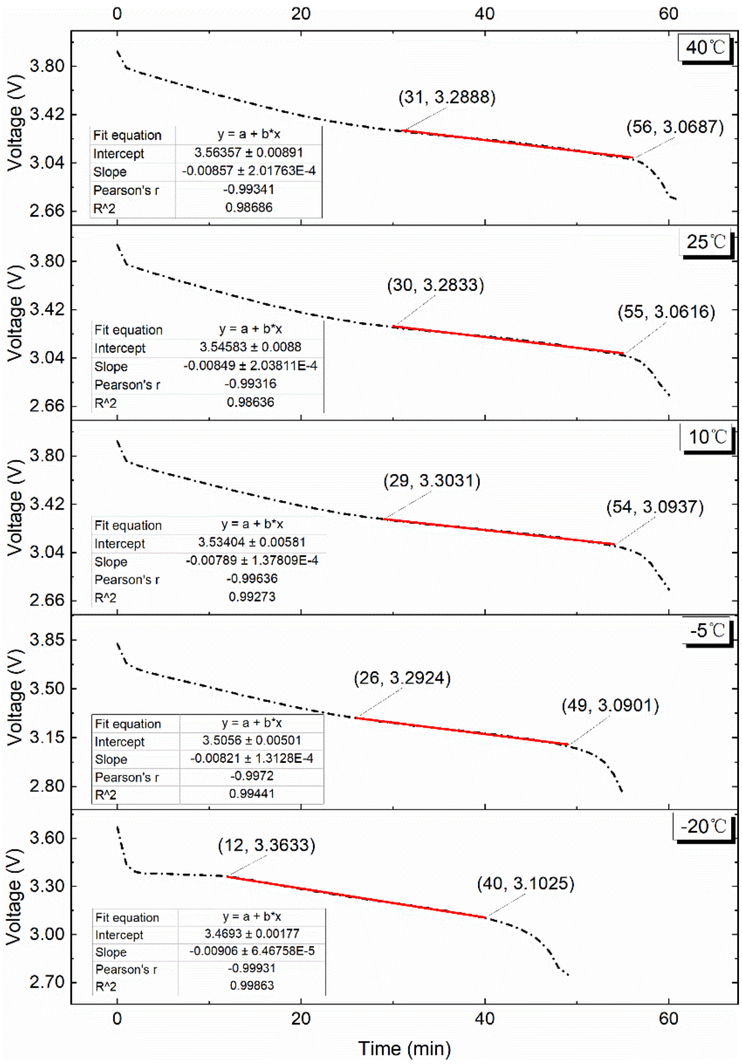

Figure 15. Influence rule of different ambient temperatures on voltage plateau period during 1C discharge.

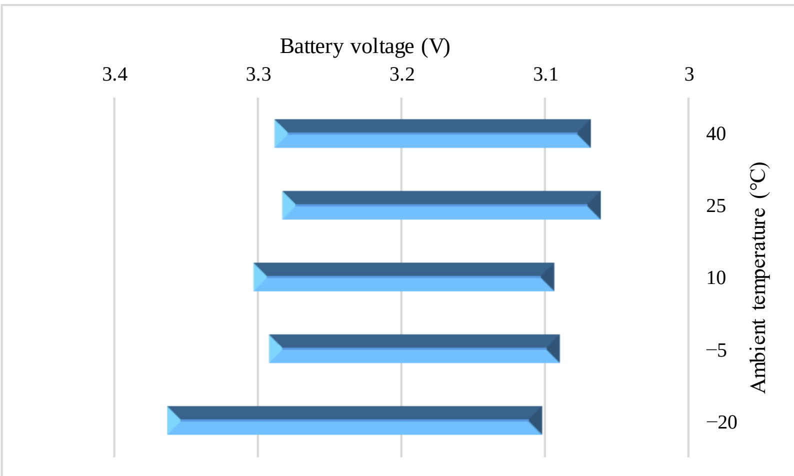

Figure 16. The voltage variation interval diagram of the voltage plateau period during 1C discharge.

4.3. Research on Battery Temperature Rise during Voltage Plateau

The comparison of the maximum temperature difference on the surface of the battery during the discharge phase is shown in Figure 17, which generally satisfies the law that the lower the ambient temperature, the greater the discharge rate, and the greater the temperature difference. At the ambient temperature of 40 °C and the discharge rate of 0.1C, the battery surface temperature difference is only 0.86 °C; at the ambient temperature of −20 °C and the discharge rate of 1C, the battery surface temperature difference reaches 14.68 °C, which is 17 times the minimum value. The temperature rise of lithium batteries at low temperature is greater than that at high temperature, mainly because the viscosity of the electrolyte increases at low temperature, and the diffusion and migration speed of lithium-ions slows down, thereby causing the internal resistance of the battery to increase. The heat generation rate of the lithium battery during operation is proportional to the battery internal resistance. Therefore, the increase of the battery internal resistance at low temperature results in more heat generation and a higher temperature rise of the battery [40,41].

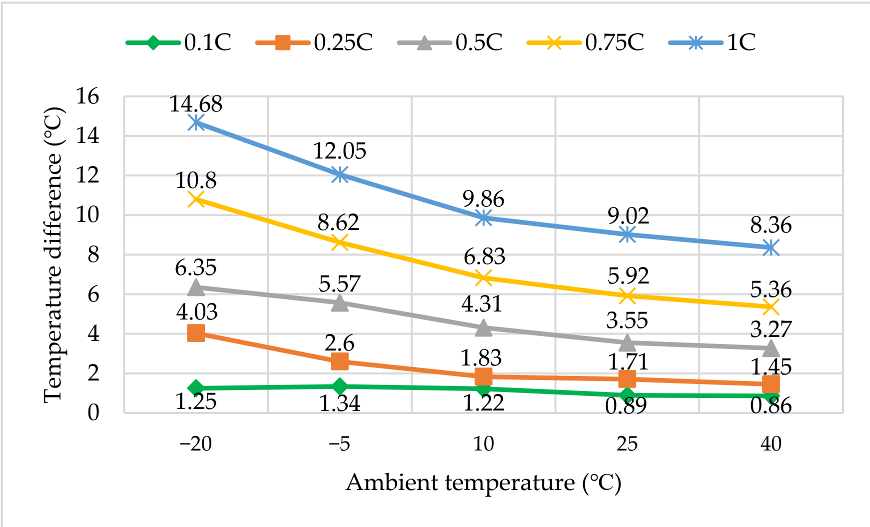

Figure 17. Comparison of the maximum temperature difference on the surface of the battery during discharge.

It is found that the temperature rise on the surface of the battery during the voltage plateau period under each experimental condition is small and does not reach the peak temperature. The phase temperature rise at the ambient temperature of −20 °C and the discharge rate of 1C only accounts for 26% of the maximum temperature difference, indicating that the battery temperature change in the voltage plateau period is relatively stable, and it is not easy to cause abnormal phenomena such as thermal runaway.

4.4. Comparison of Discharge Energy in Voltage Plateau Period

Table 3 compares and analyzes the stage discharge energy of the voltage plateau period under different experimental conditions, and judges the fitting accuracy by calculating the sample standard deviation σ of the experimental result ΔE_t and the fitting result ΔE_f. The calculation formulas of ΔE_t and ΔE_f are Formulas (1) and (2), respectively.

$$\Delta E_t = E_{t2} - E_{t1} \tag{1}$$

$$\Delta E_f = I \cdot \int_{t1}^{t2} U dt \tag{2}$$

Table 3. Comparison of discharge energy in voltage plateau period.

Discharge Rate	Ambient Temperature (°C)	ΔEt (Wh)	ΔEf (Wh)	σ (Wh)	Fitting Accuracy (%)
0.1C	40	73.89	73.87	0.0141	99.9729
	25	73.02	72.96	0.0424	99.9178
	10	70.56	70.49	0.0495	99.9007
	−5	64.88	64.95	0.0495	99.8922
	−20	37.83	37.80	0.0212	99.9206
0.25C	40	70.53	70.44	0.0636	99.8722
	25	69.75	69.82	0.0495	99.8997
	10	62.39	62.49	0.0707	99.8400
	−5	53.66	53.62	0.0283	99.9254
	−20	32.61	32.65	0.0283	99.8775
0.5C	40	65.38	65.31	0.0495	99.8928
	25	67.94	68.03	0.0636	99.8677
	10	57.91	57.85	0.0424	99.8963
	−5	50.72	50.65	0.0495	99.8618
	−20	30.22	30.24	0.0141	99.9339
0.75C	40	63.40	63.45	0.0354	99.9212
	25	63.48	63.50	0.0141	99.9685
	10	52.69	52.74	0.0354	99.9052
	−5	44.37	44.39	0.0141	99.9549
	−20	35.60	35.60	0.0000	100.0000
1C	40	53.22	53.12	0.0707	99.8117
	25	53.14	53.15	0.0071	99.9812
	10	53.45	53.38	0.0495	99.8689
	−5	48.99	49.10	0.0778	99.7760
	−20	60.27	60.38	0.0778	99.8178

In the formula, E_{t1} and E_{t2} are the discharge energy data derived from the experimental test platform at the beginning and end of the voltage plateau period, respectively.

It can be seen that the sample standard deviation σ is less than 0.08 Wh. The fitting result error is small, and the fitting equation is highly reliable. In the stage of the voltage plateau period, the discharge energy decreases with the decrease of the ambient temperature and the increase of the current rate. At any current rate, the energy at ambient temperatures of 25 °C and 40 °C is almost the same, while the energy at the ambient temperature of −20 °C is only about 50% of their energy, and the impact of low temperature on energy loss is particularly obvious [42].

5. Conclusions

Electric vehicles have a promising development prospect. As its core component, lithium-ion power battery plays a crucial role in different application scenarios. Aiming at the availability and safety of square ternary lithium batteries at different ambient temperatures and current rates, the charge-discharge cycle experiments are carried out to study the voltage, temperature, and capacity changes of lithium batteries. The voltage plateau characteristics of lithium batteries in different working states are explored, and the conclusions are as follows:

(1) Consistent with the trend of the overall discharge curve, the time and energy of the voltage plateau period decrease with the decrease of the ambient temperature and the increase of the current rate. At any current rate, the voltage plateau periods at ambient temperatures of 25 °C and 40 °C basically coincide, while at the ambient temperature of −20 °C, various indicators drop significantly. Compared with other ambient temperatures, the voltage platform is reduced by about 0.2 V, and the discharge capacity is reduced by about 50%. The low temperature environment has a significant impact on the battery

performance during the voltage plateau period. It should be avoided that the battery works for a long time under extreme low temperature conditions to reduce energy loss.

(2) At ambient temperatures of −5 °C, 10 °C, 25 °C, and 40 °C, when discharging at the current rate of 0.1C, 0.25C, 0.5C, 0.75C, and 1C, the voltage drops from 3.7 V to 3.4 V, 3.65 V to 3.35 V, 3.55 V to 3.25 V, 3.45 V to 3.2 V, and 3.3 V to 3.05 V, respectively. During this period, the battery terminal voltage changes gently, the surface temperature rise does not reach the peak, and the discharge capacity accounts for about 50%. It can be found that the battery performance at this stage is better, which provides a basis for allocating the best working section of the battery when establishing the physical model and designing the control strategy.

(3) At the ambient temperature of −20 °C, the heat generated by the initial temperature rise of the battery melts the electrolyte, increases the conductivity of the electrolyte, reduces the electron flow resistance, and makes the discharge capacity account for the highest proportion at the stage from the open circuit voltage to the initial voltage of the plateau period. The discharge capacity at the voltage plateau period only accounts for 30–35%, indicating that the performance of the voltage plateau period is not outstanding at low temperature.

Subsequent research should simultaneously carry out segmental fitting analysis and multi-angle comparison in the three periods of voltage change during the charging and discharging process, hoping to establish a more accurate battery physical model through parameter identification. Further, more work in the future should focus on the environmental reliability of lithium batteries under extreme temperature conditions.

Author Contributions: Conceptualization, X.W. and Y.Z. (Yu Zhu); methodology, X.W. and. H.N.; software and validation, Y.Z. (Yujie Zhang) and S.L.; formal analysis, X.W. and Y.Z. (Yu Zhu); investigation, X.W. and F.Z.; resources, H.N. and Y.Y.; data curation, Y.Z. (Yujie Zhang) and Y.D.; writing—original draft preparation, X.W. and Y.Z. (Yujie Zhang); writing—review and editing, Y.Z. (Yu Zhu) and Y.D.; visualization, X.W. and Y.Z. (Yujie Zhang); supervision, H.N. and Y.Y.; project administration, Y.D. and Y.Y.; funding acquisition, H.N. and Y.Y. All authors have read and agreed to the published version of the manuscript.

Funding: This research was funded by the National Natural Science Foundation of China, grant numbers 51905361 and 51876133; the Jiangsu Provincial Key Research and Development Program of China, grant number BE2021065.

Institutional Review Board Statement: Not applicable.

Informed Consent Statement: Not applicable.

Data Availability Statement: Not applicable.

Acknowledgments: This research was funded by the National Natural Science Foundation of China, grant numbers 51905361 and 51876133, the Jiangsu Provincial Key Research and Development Program of China, grant number BE2021065, and is a project funded by the Priority Academic Program Development of Jiangsu Higher Education Institutions (PAPD). The authors would like to thank the anonymous reviewers for their reviews and comments.

Conflicts of Interest: The authors declare no conflict of interest.

References

1. Li, Z.H.; Khajepour, A.; Song, J.C. A comprehensive review of the key technologies for pure electric vehicles. *Energy* **2019**, *182*, 824–839. [CrossRef]
2. Nian, V.; Hari, M.P.; Yuan, J. A new business model for encouraging the adoption of electric vehicles in the absence of policy support. *Appl. Energy* **2019**, *235*, 1106–1117. [CrossRef]
3. Harper, G.; Sommerville, R.; Kendrick, E.; Driscoll, L.; Slater, P.; Stolkin, R.; Walton, A.; Christensen, P.; Heidrich, O.; Lambert, S.; et al. Recycling lithium-ion batteries from electric vehicles. *Nature* **2019**, *575*, 75–86. [CrossRef] [PubMed]
4. Lai, X.; Chen, Q.W.; Tang, X.P.; Zhou, Y.Q.; Gao, F.R.; Guo, Y.; Bhagat, R.; Zheng, Y.J. Critical review of life cycle assessment of lithium-ion batteries for electric vehicles: A lifespan perspective. *eTransportation* **2022**, *12*, 100169. [CrossRef]
5. Yang, Z.G.; Zhang, J.L.; Kintner-Meyer, M.C.W.; Lu, X.C.; Choi, D.; Lemmon, J.P.; Liu, J. Electrochemical energy storage for green grid. *Chem. Rev.* **2011**, *111*, 3577–3613. [CrossRef] [PubMed]

6. Goodenough, J.B.; Kim, Y. Challenges for rechargeable Li batteries. *Chem. Mater.* **2010**, *22*, 587–603. [CrossRef]
7. Liu, L.; Lin, C.J.; Fan, B.; Wang, F.; Lao, L.; Yang, P.X. A new method to determine the heating power of ternary cylindrical lithium ion batteries with highly repeatable thermal runaway test characteristics. *J. Power Sources* **2020**, *472*, 228503. [CrossRef]
8. Wu, X.G.; Lv, S.Y.; Chen, J.Z. Determination of the optimum heat transfer coefficient and temperature rise analysis for a lithium-ion battery under the conditions of Harbin city bus driving cycles. *Energies* **2017**, *10*, 1723. [CrossRef]
9. Graham, J.D.; Rupp, J.A.; Brungard, E. Lithium in the green energy transition: The quest for both sustainability and security. *Sustainability* **2021**, *13*, 11274. [CrossRef]
10. Ohzuku, T.; Brodd, R.J. An overview of positive-electrode materials for advanced lithium-ion batteries. *J. Power Sources* **2007**, *174*, 449–456. [CrossRef]
11. Xiao, Z.L.; Liu, P.; Song, L.B.; Cao, Z.; Du, J.L.; Zhou, C.F.; Jiang, P. The correlation between structure and thermal properties of nickel-rich ternary cathode materials: A review. *Ionics* **2021**, *27*, 3207–3217. [CrossRef]
12. Shao, Y.J.; Huang, B.; Liu, Q.B.; Liao, S.J. Preparation and modification of Ni-Co-Mn ternary cathode materials. *Prog. Chem.* **2018**, *30*, 410–419.
13. Williard, N.; He, W.; Hendricks, C.; Pecht, M. Lessons learned from the 787 Dreamliner issue on lithium-ion battery reliability. *Energies* **2013**, *6*, 4682–4695. [CrossRef]
14. Iqbal, N.; Lee, S. Mechanical failure analysis of graphite anode particles with PVDF binders in Li-ion batteries. *J. Electrochem. Soc.* **2018**, *165*, A1961–A1970. [CrossRef]
15. Yu, D.; Ren, D.S.; Dai, K.R.; Zhang, H.; Zhang, J.M.; Yang, B.Q.; Ma, S.J.; Wang, X.F.; You, Z. Failure mechanism and predictive model of lithium-ion batteries under extremely high transient impact. *J. Energy Storage* **2021**, *43*, 103191. [CrossRef]
16. Fleischhammer, M.; Waldmann, T.; Bisle, G.; Hogg, B.; Wohlfahrt-Mehrens, M. Interaction of cyclic ageing at high-rate and low temperatures and safety in lithium-ion batteries. *J. Power Sources* **2015**, *274*, 432–439. [CrossRef]
17. Panchal, S.; Dincer, I.; Agelin-Chaab, M.; Fraser, R.; Fowler, M. Experimental and theoretical investigations of heat generation rates for a water cooled $LiFePO_4$ battery. *Int. J. Heat Mass Transf.* **2016**, *101*, 1093–1102. [CrossRef]
18. Chen, X.; Lv, S.S.; Pei, Y.; Chen, L.; Ni, H.J. Influence of temperature on the $LiFePO_4$ power batteries' discharge voltage values. *New Chem. Mater.* **2015**, *43*, 202–203.
19. Wang, C.X. Study on Internal Thermal Strain Characteristics of Lithium Batteries at High C Rates under Low Temperature. Master's Thesis, Civil Aviation Flight University of China, Guanghan, China, 2020.
20. An, Z.J.; Jia, L.; Ding, Y.; Dang, C.; Li, X.J. A review on lithium-ion power battery thermal management technologies and thermal safety. *J. Therm. Sci.* **2017**, *26*, 391–412. [CrossRef]
21. Gu, Y.J.; Sun, X.F.; Li, Z.L.; Xu, X.M.; Chen, Y.C.; Huang, X.W.; Jiang, H.F.; Li, B.Y. Study of high and low temperature property of 10 Ah Li-ion battery. *Chin. Battery Ind.* **2009**, *14*, 223–226.
22. Liu, Z.W.; Liu, X.L.; Hao, H.; Zhao, F.Q.; Amer, A.A.; Babiker, H. Research on the critical issues for power battery reusing of new energy vehicles in China. *Energies* **2020**, *13*, 1932. [CrossRef]
23. Gantenbein, S.; Schönleber, M.; Weiss, M.; Ivers-Tiffée, E. Capacity fade in lithium-ion batteries and cyclic aging over various state-of-charge ranges. *Sustainability* **2019**, *11*, 6697. [CrossRef]
24. Situ, W.F.; Yang, X.Q.; Li, X.X.; Zhang, G.Q.; Rao, M.M.; Wei, C.; Huang, Z. Effect of high temperature environment on the performance of $LiNi_{0.5}Co_{0.2}Mn_{0.3}O_2$ battery. *Int. J. Heat Mass Transf.* **2017**, *104*, 743–748. [CrossRef]
25. Bloom, I.; Walker, L.K.; Basco, J.K.; Abraham, D.P.; Christophersen, J.P.; Ho, C.D. Differential voltage analyses of high-power lithium-ion cells. 4. Cells containing NMC. *J. Power Sources* **2010**, *195*, 877–882. [CrossRef]
26. Jia, X.L. The Study on Estimation Method about the Capacity of Power Lithium-Ion Battery. Master's Thesis, Shenzhen Graduate School, Harbin Institute of Technology, Shenzhen, China, 2016.
27. Zhang, Y.P.; Wu, L.L.; Zhao, J.B.; Yu, W.Y. A facile precursor-separated method to synthesize nano-crystalline $LiFePO_4$/C cathode materials. *J. Electroanal. Chem.* **2014**, *719*, 1–6. [CrossRef]
28. Erdinc, O.; Vural, B.; Uzunoglu, M. A dynamic lithium-ion battery model considering the effects of temperature and capacity fading. In Proceedings of the 2009 International Conference on Clean Electrical Power IEEE, Capri, Italy, 9–11 June 2009; pp. 383–386.
29. Gholami, J.; Barzoki, M.F. Electrochemical modeling and parameter sensitivity of lithium-ion battery at low temperature. *J. Energy Storage* **2021**, *43*, 103189. [CrossRef]
30. Li, C.L.; Cui, N.X.; Wang, C.Y.; Zhang, C.H. Simplified electrochemical lithium-ion battery model with variable solid-phase diffusion and parameter identification over wide temperature range. *J. Power Sources* **2021**, *497*, 229900. [CrossRef]
31. Minato, T.; Abe, T. Surface and interface sciences of Li-ion batteries: Research progress in electrode electrolyte interface. *Prog. Surf. Sci.* **2017**, *92*, 240–280. [CrossRef]
32. Ma, S.; Jiang, M.D.; Tao, P.; Song, C.Y.; Wu, J.B.; Wang, J.; Deng, T.; Shang, W. Temperature effect and thermal impact in lithium-ion batteries: A review. *Prog. Nat. Sci. Mater. Int.* **2018**, *28*, 653–666. [CrossRef]
33. Jiang, C.; Wang, S.L.; Wu, B.; Fernandez, C.; Xiong, X.; Coffie-Ken, J. A state-of-charge estimation method of the power lithium-ion battery in complex conditions based on adaptive square root extended Kalman filter. *Energy* **2021**, *219*, 119603. [CrossRef]
34. Wang, S.L.; Stroe, D.; Fernandez, C.; Yu, C.M.; Zou, C.Y.; Li, X.X. A novel energy management strategy for the ternary lithium batteries based on the dynamic equivalent circuit modeling and differential Kalman filtering under time-varying conditions. *J. Power Sources* **2020**, *450*, 227652. [CrossRef]

35. Liu, X. Test Bench Establishing and Nonlinear Modeling of Lithium-Ion Battery and Supercapacitor. Master's Thesis, Wuhan University of Technology, Wuhan, China, 2019.
36. Li, B.; Xia, D.G. Anionic redox in rechargeable lithium batteries. *Adv. Mater.* **2017**, *29*, 1701054. [CrossRef] [PubMed]
37. Lv, S.S.; Wang, X.X.; Lu, W.F.; Zhang, J.Q.; Ni, H.J. The influence of temperature on the capacity of lithium ion batteries with different anodes. *Energies* **2021**, *15*, 60. [CrossRef]
38. Lux, S.F.; Schmuck, M.; Appetecchi, G.B.; Passerini, S.; Winter, M.; Balducci, A. Lithium insertion in graphite from ternary ionic liquid–lithium salt electrolytes: II. Evaluation of specific capacity and cycling efficiency and stability at room temperature. *J. Power Sources* **2009**, *192*, 606–611. [CrossRef]
39. Wang, X.X.; Zhang, Y.J.; Zhu, Y.; Lv, S.S.; Ni, H.J.; Deng, Y.L.; Yuan, Y.N. Effect of different hot-pressing pressure and temperature on the performance of titanium mesh-based MEA for DMFC. *Membranes* **2022**, *12*, 431. [CrossRef]
40. Lei, Z.G.; Zhang, Y.W.; Lei, X.G. Temperature uniformity of a heated lithium-ion battery cell in cold climate. *Appl. Therm. Eng.* **2018**, *129*, 148–154. [CrossRef]
41. Wang, X.X.; Liu, S.R.; Zhang, Y.J.; Lv, S.S.; Ni, H.J.; Deng, Y.L.; Yuan, Y.N. A review of the power battery thermal management system with different cooling, heating and coupling system. *Energies* **2022**, *15*, 1963. [CrossRef]
42. Lai, X.; Huang, Y.F.; Gu, H.H.; Han, X.B.; Feng, X.N.; Dai, H.F.; Zheng, Y.J.; Ouyang, M.G. Remaining discharge energy estimation for lithium-ion batteries based on future load prediction considering temperature and ageing effects. *Energy* **2022**, *238*, 121754. [CrossRef]